UNIVERSIDAD SAN FRANCISCO DE QUITO USFQ

Colegio de Ciencias Biológicas y Ambientales

Combatting Drug Resistance: Exploring Novel Schiff Bases Against Resistant Biofilms

Tamia Xaymara Iza García
Biotecnología

Trabajo de fin de carrera presentado como requisito
para la obtención del título de
Ingeniera Biotecnóloga

Quito, 20 de diciembre de 2023

UNIVERSIDAD SAN FRANCISCO DE QUITO USFQ

Colegio de Ciencias Biológicas y Ambientales

HOJA DE CALIFICACIÓN
DE TRABAJO DE FIN DE CARRERA

Combatting Drug Resistance: Exploring Novel Schiff Bases Against Resistant Biofilms

Tamia Xaymara Iza García

Nombre del profesor, Título académico **Antonio Machado, PhD. en Ingeniería Biomédica**

Quito, 20 de diciembre de 2023

© DERECHOS DE AUTOR

Nombres y apellidos: Tamia Xaymara Iza García

Código: 00213080

Cédula de identidad: 1751337765

Lugar y fecha: Quito, 20 de diciembre de 2023

ACLARACIÓN PARA PUBLICACIÓN

Nota: El presente trabajo, en su totalidad o cualquiera de sus partes, no debe ser considerado como una publicación, incluso a pesar de estar disponible sin restricciones a través de un repositorio institucional. Esta declaración se alinea con las prácticas y recomendaciones presentadas por el Committee on Publication Ethics COPE descritas por Barbour et al. (2017) Discussion document on best practice for issues around theses publishing, disponible en http://bit.ly/COPETheses.

UNPUBLISHED DOCUMENT

Note: The following capstone project is available through Universidad San Francisco de Quito USFQ institutional repository. Nonetheless, this project – in whole or in part – should not be considered a publication. This statement follows the recommendations presented by the Committee on Publication Ethics COPE described by Barbour et al. (2017) Discussion document on best practice for issues around theses publishing available on http://bit.ly/COPETheses.

RESUMEN

Las principales causas de la resistencia a los antimicrobianos (AMR) son el uso indebido de antibióticos, la mala gestión de residuos y la rápida capacidad de evolución de las bacterias. La AMR suele estar inducida por varios factores de virulencia,

La presencia de genes de resistencia transferibles y la capacidad de formar biopelículas son dos factores de virulencia. Debido a la lentitud en el desarrollo de nuevos fármacos, los investigadores se han visto obligados a buscar alternativas a los antibióticos. Una de estas es el uso de bases de Schiff, compuestos que contienen azomethinas con amplia variedad estructural y que se ha descrito que poseen actividad biológica. En este trabajo, evaluamos la actividad anti-biopelícula de ocho bases de Schiff (3a-3h) derivadas de la 4-aminoantipirina con diferentes cinamaldehídos, analizando la inhibición de la formación de biopelículas y la capacidad de erradicación en biopelículas maduras formadas después de 24 horas, de *S. aureus* MRSA 333, *K. pneumoniae* KPC 609803, *P. aeruginosa* P28, *E. faecalis* INSPI 032 y *C. albicans* INSPI, considerados patógenos clínicamente relevantes. Se observó un rango de inhibición de la biomasa del 0,56% al 48,47%, donde los compuestos 3a, 3f y 3d mostraron los mejores efectos, mientras que para la erradicación se encontró un rango del 3,36% al 31,91%, siendo los compuestos 3a y 3h los mejores. El ensayo de viabilidad celular realizado después de los ensayos de inhibición demostró la reducción del número total de células entre un 3,78% y un 74,94%, además de generar una mortalidad de hasta un 94,60%. Cada compuesto presentó una actividad específica para cada patógeno, lo que debe tenerse en cuenta para futuros estudios.

Palabras-clave: Biopelículas, resistencia antibacteriana, bases Schiff, microscopía de fluorescencia, actividad antibiofilm.

ABSTRACT

The main causes of antimicrobial resistance (AMR) are the misuse of antibiotics, problems with improper waste management, and the ability of bacteria to rapidly evolve. AMR is commonly induced by several virulence factors, the presence of resistance genes that can be transferred, and the ability to form biofilms, which is considered to be one main virulence factor. Biofilms are microbial communities embedded in extracellular matrices and undergoing a phenotypic shift. Due to the slow development of new drugs, researchers have been led to search for alternatives to antibiotics. One of the alternative treatments is the use of Schiff bases, compounds that contain azamethines with a wide structural variety, which have been reported to have biological activity. In the present work, we evaluated the antibiofilm activity of eight Schiff bases (3a-3h) derived from 4-aminoantipyrine with different cinnamaldehydes, by analyzing the inhibition of biofilm formation, and the eradication capacity in mature biofilm formed after 24 hours, of *S. aureus* MRSA 333, *K. pneumoniae* KPC 609803, *P. aeruginosa* P28, *E. faecalis* INSPI 032, and *C. albicans* INSPI, which are considered to be clinically relevant pathogens. A range of biomass inhibition from 0.56% to 48.47% was found, where compounds 3a, 3f, and 3d showed the best effects, while for eradication a range of 3.36% to 31.91% was found, with compounds 3a and 3h being the best. The live/dead assay performed after inhibition assays demonstrated the reduction of total number of cells by 3.78% and 74.94%, in addition to generating a mortality of up to 94.60%. Each compound had a specific activity for each pathogen, which should be considered for future studies.

Keywords: Biofilms, antibacterial resistance, Schiff bases, fluorescence microscopy, antibiofilm activity.

TABLE OF CONTENTS

TABLE INDEX

INDEX OF FIGURES

INDEX OF APPENDICES

INTRODUCTION

In a scenario in which bacteria evolve rapidly in the face of overexposure to antimicrobials, becoming therefore resistant or tolerant by resisting the biological activity of these drugs or generating defense mechanisms, antimicrobial resistance (AMR) has become a global problem (Chung et al., 2021). It was estimated that in 2019 worldwide about 4.95 million deaths were directly associated with drug-resistant infections, of which 1.27 million are directly attributable to resistance, becoming the third leading cause of death in that year. At the level of America Latin (Annex A), 57.9 per 100,000 deaths are associated with multidrug resistance (MDR) and 14.4 per 100,000 are attributable to resistance (Murray et al., 2022). Also, Chinemerem Nwobodo and colleagues estimated that this type of infection will claim up to 10 million lives per year by 2050 (Chinemerem Nwobodo et al., 2022). These problems are directly related to the misuse and abuse of antibiotics, and it has been shown that developing countries tend to develop increased resistance to antibacterials due to factors related to poor health care, agriculture, poor waste management, and inappropriate prescribing patterns (Salam et al., 2023). The principal sources and routes of transmission of AMR are the human interface, animals, and the environment, which constitutes a reservoir of resistance genes (Salam et al., 2023).

One of the principal factors of virulence mechanisms is the ability to produce biofilm as a multicellular community composed of mono- or multispecies microorganisms. The biofilms are characterized by the presence of the highly dense extracellular matrix in which bacteria are embedded. This gives them the ability to survive in hostile environments with few resources, mechanic forces, competitors, and toxic elements (Machado et al., 2023a). The process of biofilm formation occurs in four

essential steps, the migration of cells for their initial reversible adhesion to the surfaces, colonization with irreversible adhesion, its evolution into microcolonies with extracellular polymeric substance (EPS) production, and the maturation of biofilm with cellular stratification and phenotypic shift until dispersion stage with the detachment of cells for the colonization of new surfaces (Vani et al., 2023). Although it is well known the common mechanisms of the resistance in the planktonic growth stage such as mutation, change in cellular permeability, and several efflux systems. In biofilm, the mechanisms of resistance are associated with the low penetration of antibiotics in the matrix, a different chemical microenvironment, and different metabolic subpopulation estates known as latent or persistent cells (Sharma et al., 2019).

At the clinical level, it has been found that between 65% and 85% of microbial infections are associated with the formation of biofilms (Machado et al., 2023a). Moreover, hospital equipments, such as pacemakers and peripheral catheters, have been reported as surfaces of easy colonization and biofilm formation leading to nosocomial or hospital-acquired infections in immunocompromised patients (Vani et al., 2023). The most prevalent biofilms in hospital-acquired infections are *Staphylococcus aureus* (including MRSA), *Escherichia coli*, *Klebsiella pneumoniae*, and *Candida albicans* (Cangui-Panchi et al., 2022). Concerning the immune system, certain well-known pathogens demonstrated the potential to efficiently evade the immune responses and spread to various tissues, more exactly *Pseudomonas aeruginosa*, *Staphylococcus* species, and *Candida* species. Several properties have been observed in these pathogen-associated biofilms such as quorum sensing, cellular communication to interfere with phagocytosis recruitment, blocking immunoglobulin pathways, and even complement components (Cangui-Panchi et al., 2023). Other virulence factors have also been reported such as the prevention of bacterial recognition, iron acquisition systems, and host cellular

damage through the production of different types of proteinases (Cangui-Panchi et al., 2023).

The serious public health problem caused by AMR and biofilm formation led to the search for alternative treatments to classical antibiotics and the low number of new antibiotics developed by the pharmaceutical industry as they do not invest due to the rapid appearance of resistance, which makes it unreliable (Chinemerem Nwobodo et al., 2022). One of the most novel alternative treatments is the Schiff bases being compounds that contain azomethine in their structure and known for their versatility for imines, chemically, these compounds have basic properties that will decrease with hybridization processes with the imine (Tuna Subasi, 2023). Schiff bases can make highly stable structures with 4, 5, and 6 rings by donating more than one pair of electrons (Tuna Subasi, 2023). This versatility allows these compounds to react with aldehydes, ketones, and carboxylic compounds, becoming also able to incorporate metal ions and opening a window of opportunity for the diversification of its structure (Tsacheva et al., 2023). The first method used for the formation of bases is the synthesis by reaction of carbonyl compounds with primary imines. Within the formation reaction, it is dependent on the pH which must be between 3 and 4 (Tuna Subasi, 2023). Currently, the main synthesis techniques commonly employed solvent-free irradiation, molecular sieves, and microwave irradiation in short periods of time (Tsacheva et al., 2023). It is these chemical characteristics and their structural versatility that result in the bases having different biological effects, the main effect is due to the role of bases, as intermediates during the biosynthesis of alpha-amino acids (Tuna Subasi, 2023). Among the main biological activities are the antimalarial activity with 5-nitroisoquinoline derivatives with application doses like the standard treatment, the antifungal activity becoming more potent than fluconazole agent for phytopathogenic fungi and clinically relevant fungi

serving as fungicides or as growth inhibitors, the antiviral activity where salicylaldehyde-derived bases have been effective against viruses (such as hepatitis viruses) showing inhibition of viral growth through in vivo assays, and anticancerogenic agents because bases serve as pre-cursors for polyamines or copolymers that have been used as chemotherapeutics (Da Silva et al., 2011; Tsacheva et al., 2023). The most important in this study is the antibacterial activity, numerous studies using different resources for Schiff bases have been published in the last 10 years (Ceramella et al., 2022). Among the most active compounds reported are metal-bound bases. Studies reported bases derived from aminoprazoles with activity against multidrug-resistant (MDR) bacteria, and the activity is related to DNA or enzyme binding capacity (Ceramella et al., 2022). In some cases, the antibacterial activity is equal or superior to commercial antibiotics (Srinivasan et al., 2021). Concerning studies about antibiofilm activity by Schiff bases, only a few studies have been published in recent years (Arshia et al., 2017; Elmehbad et al., 2022; Biswas et al., 2023), as it is shown in Annex B.

Therefore, the present study aimed to further evaluate the antibiofilm activity of Schiff base derivatives from 4-aminoantipyrine with different cinnamaldehydes against several well-known biofilm-forming pathogens of clinical relevance, more exactly *S. aureus* MRSA 333, *K. pneumoniae* KPC 609803, *P. aeruginosa* P28, *E. faecalis* INSPI 032, and *C. albicans* INSPI. Antibiofilm activity was studied during the biofilm establishment phase with inhibition assays, and against mature biofilms with eradication assays, to further evaluate the status of bacteria within the biofilm, live and dead analysis was also performed.

METHODS

Synthesis of Schiff bases

All solvents and reagents were from Aldrich Group Ltd. (St. Louis, MO, USA). All melting points (MPs) were determined on a Fisher-Johns analog melting point apparatus to measure the MPs of the Schiff bases. Fourier transform infrared (FTIR) spectra were recorded by a Perkin Elmer FTIR Spectrum One by using an ATR system (4000–650 cm^{-1}). The 1H and 13C nuclear magnetic resonance (NMR) spectra were recorded at 298 K on a Bruker Advance 500 MHz spectrometer equipped with a z-gradient and triple-resonance (1H, 13C, 15N) cryoprobe using DMSO-d6 or CDCl3 as solvents. Chemical shifts are expressed in parts per million (ppm) with tetramethylsilane (TMS) as an internal reference (TMS, $\delta = 0$ ppm) for protons. Reactions were monitored by thin layer chromatography (TLC) on silica gel using ethyl acetate/hexane mixtures as a solvent and compounds visualized by ultraviolet (UV) lamp. All Schiff bases were synthesized according to the reported procedures by our collaboration research group (Teran et al., 2019).

Antibiofilm activity

In the biofilm inhibition assays, 190 µL of a bacterial suspension in Mueller Hinton Broth (MHB) at 10^8 colony-forming units (CFU)/mL was introduced into 96-well flat bottom plates from Tecan Group Ltd. (Mannedorf, Switzerland). To this, 10 µL of concentrated Schiff bases were added, achieving the final concentrations of 10 and 100 µM within wells of the 96-well plate. The plates were then placed in an incubator at 37 ºC under aerobic conditions for 24 h in the biofilm inhibition assays. Concerning biofilm eradication assays, an identical bacterial inoculum in MHB was placed in 96-well plates and then incubated for 48 h at 37 ºC under aerobic conditions before the treatment with

Schiff bases. After this incubation period, the MHB was removed from the wells, and washing steps using phosphate-buffered saline (PBS, at pH 7.4) were conducted. The fully formed biofilms were then treated with Schiff bases at final concentrations of 10 and 100 μM in fresh media, and the plates were again incubated at 37 ºC under aerobic conditions for 24 h (Fernandez-Soto et al., 2023; Teran et al., 2019). At the end of inhibition and eradication assays, all plates were washed three times with PBS after the media was removed. Each biofilm sample was fixed using 200 μL of methanol (99% v/v; Sigma-Aldrich, St. Louis, MO, USA) for 15 minutes and crystal violet (CV) staining (0.1% w/v; Sigma-Aldrich, St. Louis, MO, USA) was realized for 10 minutes, followed by four washes with distilled water. Biofilm dissolution was achieved using ethanol (95% v/v; Sigma-Aldrich, St. Louis, MO, USA), and the extent of biofilm formation was measured using spectrophotometry in the ELISA Elx808 spectrophotometer (BioTek, Winooski, GU, USA) at an optical density of 570 nm. Finally, the percentage of biofilm inhibition and eradication was determined as previously outlined (Rakhmawatie et al., 2019; Patel et al., 20211; Fernandez-Soto et al., 2023; Sornsenee et al., 2021). All assays contained positive controls involving bacterial growth in media only and negative control consisting of media with bacterial growth plus a solution of 2.5% dimethyl sulfoxide (DMSO) without Schiff bases. Additionally, a well-containing medium devoid of any bacterial inoculum was employed to serve as a sterility control. All assays were conducted with triplicate controls/samples across a minimum of two independent experiments.

Fluorescence Staining

All biofilm samples were further analyzed by fluorescence microscopy (FM) using live/dead staining. After each biofilm formation assay in 96-well plates at the same biofilm experimental settings previously described. A working solution of fluorescent

stains was prepared by adding 1.0 mL of SYTO® 9 stain and 10 μL of propidium iodide (PI) stain (FilmTracer™ LIVE/DEAD® Biofilm Viability Kit), mixed in the proportion 1:100 of PI/SYTO-9, into 10 mL of filter-sterilized water in a foil-covered container. About 100 μL of the live/dead working solution was added onto biofilm samples and were then incubated for 15-30 min at room temperature, protected from light. Finally, FM analysis was carried out using an Olympus BX50 microscope (Olympus Corporation, Tokyo, Japan) equipped with a 100x oil immersion objective. Images were captured with AmScope Digital Camera MU633-FL (AmScope, California, USA) and digitalized with AmScope software version 1.2.2.10. As previously described (Rosenberg et al., 2019), for counting purposes at least 15 images were taken per sample on the 22-mm diameter glass coverslip at random locations. These results were expressed as the number of cells ± standard deviation per cm^2 (N. of cells/cm^2 ± SD). The percentages of dead and alive cells within images were measured through ImageJ version 1.57 by Fiji (Schindelin et al., 2012) using the macros Biofilms Viability checker (Mountcastle et al., 2021).

Statistical analyses

All data of the present study were further evaluated by statistical analyses. Due to the non-normal distribution of the data set, a non-parametric test was applied, more exactly the Wilcoxon nonparametric test was used for pairwise comparison between control and treated samples in both biofilm inhibition and eradication assays. Statistical analyses were realized in R studio version 4.0 (https://www.rstudio.com/products/rstudio/download/) using several R packages ("ggpubr", "rstatixs", "openxlsx" and the "tidyverse" set of packages) (Kassambara, 2021; Wickham et al., 2019). Finally, all p-values <0.05 were considered significant.

RESULTS

Antibiofilm activity evaluation

The impact of the synthesized Schiff bases was investigated against different biofilm-forming multidrug-resistant pathogens (see Tables 1 and 2). These evaluations were conducted using compounds 3a-h (see Figure 1) at concentrations of 10 and 100 µM against *S. aureus* MRSA 333, *K. pneumoniae* KPC 609803, *P. aeruginosa* P28, *E. faecalis* INSPI 032, and *C. albicans* INSPI.

An assessment of non-normal distribution and non-parametric Wilcoxon testing was applied to compare the treatment outcomes with the DMSO control after evaluating its antibiofilm activity against and the positive control (i.e., pathogen growth in only medium culture). Wilcoxon test was used for biofilm inhibition and eradication assays. No significant differences were observed in antibiofilm activities at both assays between 10 and 100 µM concentrations of the Schiff bases 3a–h compounds, as shown in Tables 1 and 2.

Biofilm inhibition activity

Our results demonstrated the ability to inhibit biofilm formation by all Schiff bases ranging between 0.56% and 48.47% when counteracted by the effect of the solvent (DMSO controls) used to dissolve the Schiff bases, as shown in Figure 2. Similarly, DMSO controls displayed biofilm inhibition within a range of 1.78% to 23.03% across all pathogens. When compared to the positive control, statistical differences were observed for all pathogens (p-values <0.01), except for *E. faecalis* INSPI 032 (see Table 1). The maximum inhibition activities were observed by Schiff base 3f compound against *P. aeruginosa* P28 with 48.47% biofilm inhibition and *C. albicans* INSPI with 36.48%.

Next, Schiff base 3a compound also showed maximum inhibition activities against *K. pneumoniae* KPC 609803 and S. *aureus* MRSA 333 with 40.51% and 29.97% of biofilm inhibition, respectively. Finally, the Schiff base 3d compound demonstrated greater biofilm inhibition in *E. faecalis* INSPI 032 (24.64%).

Biofilm eradication activity

The biofilm eradication ability of the Schiff bases 3a–h compounds was then evaluated on mature 48-h biofilms. As shown in Figure 3, the eradication activity ranged between 3.36% and 31.91%. Moreover, the maximum biofilm eradication activities were observed by Schiff base 3h compound against *K. pneumoniae* KPC 609803 (30.45%), *E. faecalis* INSPI 032 (21.27%), and *S. aureus* MRSA 333 (24.19%) after counteracted the DMSO controls, as shown in Table 2. Meanwhile, Schiff base 3a compound proved a fetter biofilm eradication effect against *P. aeruginosa* P28 (29.25%) and *C. albicans* INSPI (28.83%).

Total Cell and Live/Dead Cells Count in Biofilms

Further antimicrobial characterization of the best Schiff bases was realized by LIVE/DEAD staining assays using epifluorescence microscopy (see Table 3). The selection of the best Schiff bases was realized by the preliminary results obtained by biofilm inhibition assays. As shown in Table 3, a reduction in the total cell count was observed in all treated samples, when compared to positive controls. However, a significant difference between the positive control and DMSO control was observed in most cases except for *K. pneumoniae* KPC 609803 and *S. aureus* MRSA 333 when treated with Schiff base 3a compound. Due to this statistical significance in most cases, the treated samples were compared against DMSO control. Although DMSO controls showed a total cell reduction range between 0.21% and 94.13%, samples revealed greater

total cell reduction when treated with Schiff base 3f compound against *P. aeruginosa* P28 (p>0.05) and *C. albicans* INSPI (p<0.0001). While general results against the evaluated pathogens demonstrated a range of total cell reduction between 3.78% and 74.94%. Furthermore, the mortality range of the treated samples by Schiff bases after counteracting the values from DMSO control was between 21.16 and 92.60%. Schiff base 3a compound at 100 µM exhibited a potent bactericidal activity against *K. pneumoniae* KPC 609803 and *S. aureus* MRSA 333 showing 94.60 and 89.90% of dead cells within biofilms, respectively. Meanwhile, Schiff base 3f compound at 100 µM also evidenced similar bactericidal activity against *P. aeruginosa* P28 and *C. albicans* INSPI showing 94.72 and 40.0% of dead cells, respectively. At last, Schiff base 3d compound at 100 µM showed the lowest dead cell percentage against *E. faecalis* INSPI 032 (31.90%) without surpassing the mortality induced by DMSO control (36.80%).

DISCUSSION

One of the most significant virulence factors is the ability of bacteria to establish biofilms being most human infections associated with biofilm formation (Cangui-Panchi et al., 2022, 2023). The role of biofilm in antimicrobial resistance is complex and has been shown to significantly drive resistance in biofilm-associated surfaces, microenvironments, and persisted cells (Atiencia-Carrera, Cabezas-Mera et al., 2023; Machado et al., 2023). According to the World Health Organization (WHO), antimicrobial resistance has become one of the primary threats to public health (Kwon & Powderly, 2021; Reardon, 2014). More than 70% of all pathogenic bacteria are resistant to commercially available antibiotics (Chinemerem Nwobodo et al., 2022). This situation has made the search for alternative antibacterial agents a primary priority worldwide. Schiff bases, formed as a result of the nucleophilic addition reaction of aldehydes and ketones with primary amines, had been reported to possess numerous beneficial effects, such as antimalarial, antiproliferative, antiviral, and antimicrobial activity (Ceramella et al., 2022; More et al., 2013). However, when it comes to evaluating antibiofilm activity, only a few studies briefly described preliminary evaluations for future biomedical applications (Chung et al., 2021; Mastoor et al., 2022; Ceramella et al., 2022; Mohini et al., 2014). In the present study, several synthesized Schiff bases were tested against various biofilm-forming pathogens to assess their ability to inhibit and eradicate biofilms. The potential of the synthesized Schiff bases to inhibit and eradicate biofilms was confirmed in this study by biomass and LIVE/DEAD assays testing their effectiveness against a range of biofilm-forming pathogens, more exactly *S. aureus* MRSA 333, *K. pneumoniae* KPC 609803, *P. aeruginosa* P28, *E. faecalis* INSPI 032, and *C. albicans* INSPI. Biomass and dead cells evaluation demonstrated the efficiency of Schiff bases 3a,

3d, and 3f compounds showing good biofilm inhibition (1.78% to 23.03%), increase of dead cells (21.16 to 92.60 %), and total cell reduction (3.78% to 74.94%).

Each Schiff base compound of the present study exhibited different antimicrobial effects on the biofilm of each microorganism. These results were expected due to the different specificity properties of the Schiff bases compounds, being this acknowledgement crucial for the development of future pharmacological applications. Recently, Sindelo and colleagues reported the effects of Schiff-base morpholino phthalocyanines with cationic complexes against mono and multispecies biofilms formed by *C. albicans* ATCC 24433, *E. coli* ATCC 25922, *K. pneumoniae* ATCC 13883, *S. aureus* ATCC 25923, *Salmonella enterica* serovar Choleraesuis ATCC 10708, MRSA ATCC 700699, and vancomycin-resistant *Enterococcus faecium* (VREF) ATCC 51299 (Sindelo et al., 2023). Moreover, these authors demonstrated the ability of the cationic compounds to moderate the eradication of monospecies biofilms with concentrations until 200 µM. However, no biofilm inhibition assays were realized by Sindelo et al. (2023). In agreement, the present study also revealed a range of biofilm inhibition on several well-known pathogens with Schiff bases at lower concentrations (10 and 100 µM). Our results evidenced its maximum inhibition effect against *P. aeruginosa* P28 biofilms, being well characterized by its overproduction of exopolysaccharides, and the existence of multiple efflux pumps (Ciofu & Tolker-Nielsen, 2019). Teran and colleagues assessed the antibacterial activity of Schiff bases derived from the same precursor, reporting low antibacterial activity with a bacteriostatic effect (Teran et al., 2019). However, they did not evaluate the antibiofilm effects due to the low preliminary results on planktonic bacteria. The results from our study demonstrated significant biofilm inhibition properties in agreement with Amer et al. (2021). These authors reported moderate antibacterial activity of Schiff bases derived from sulfamidines against *P.*

aeruginosa biofilms. Additionally, the results on the total cell reduction and elevated number of dead cells in the present study confirmed the antibiofilm activity of the Schiff bases. Although the presence of biofilms is usually associated with multiple antimicrobial resistance through its structural protection, the present study observed a lower resistance on *K. pneumoniae* KPC 609803 biofilms, where low values of total cells were observed in biofilm formation as previously described in other studies (Cabezas-Mera et al., 2023; Cusumano et al., 2019). Even though the highest percentage of dead cells (94.6%) was obtained on *K. pneumoniae* KPC 609803 biofilms using the Schiff base 3a compound at 100 µM. Regarding *E. faecalis*, similar results were reported by Stlorcyk and colleagues showing the antimicrobial activity of Schiff bases against *E. faecalis* ATCC 29212 (Stlorcyk et al., 2021). Our study was able to reveal moderate biofilm inhibition (24.64%) and dead cells (31.89%). It has been reported that MRSA strains can form strong AMR biofilms, this ability is closely related to the presence of virulence factors, such as reported by Silva and colleagues, as there is an interaction with surface proteins, the formation of a multilayer banking, and the presence of fibrinogen binding proteins (Silva et al., 2021). As shown in Figure 2, the inhibition activity was moderated like reported by Mohini et al. (2014), where the authors used Schiff base analogues derived from methyl-12-aminooctadec-9-enoate against *S. aureus* MTCC 96, *S. aureus* MLS-16 MTCC 2940, and *Bacillus subtilis* MTCC 121. Furthermore, eradication results in the present study were moderately high and in agreement with the results reported by Chung and colleagues, where the authors tested two Cu(II) Schiff base complexes by themselves and in combination with two antibiotics (vancomycin and oxacillin) against methicillin-susceptible and resistant *S. aureus* strains (Chung et al., 2021). Finally, *C. albicans* biofilm is well-known to generate multiple resistance against antimicrobial agents due to the regulation of efflux pumps excluding numerous drugs or toxins and also being active

during the first stages of biofilm development (Gulati & Nobile, 2016). Likewise, some extracellular compounds also interfere with the mechanism of action from antifungals, and recalcitrant cells are intrinsically resistant because they are metabolically inactive (Gulati & Nobile, 2016). This study's findings align with existing resistance mechanisms. Teran et al. (2019) observed similar fungistatic effects in 4-aminoantipyrine-derived Schiff bases against *C. albicans*, suggesting a link between activity and the presence of specific functional groups. However, their study lacked biofilm assays for direct comparison. Notably, our biofilm inhibition results were moderate (biomass growth: 36.85%, dead cells: 40.02%).

Overall results evidenced good antibiofilm activity in all Schiff bases compounds demonstrating bactericidal effects through dead cells evaluation from LIVE/DEAD assays. In addition, biomass assays showed partial eradication effects against mature biofilms from all evaluated pathogens, as reported by Sindelo et al. (2023). Furthermore, as postulated by Mastoor and colleagues, the Schiff bases had the potential to highly inhibit biofilm formation by affecting several genes on the phenotypic shift of the biofilm development (Mastoor et al., 2022). However, our results showed lower values of biofilm inhibition and eradication than reported by Mastoor et al. (2022) and Sindelo et al. (2023). One plausible explanation could be the lower concentration range of Schiff bases (10 and 100 µM) used in the present study. Also, controversies about the antimicrobial activity of Schiff bases remain in the literature about their bactericidal or bacteriostatic effects (Teran et al., 2019). Therefore, future studies must be performed to further evaluate the bactericidal and/or bacteriostatic effects of Schiff bases against pathogens with additional methods, besides biomass and live/dead assays, characterizing the antimicrobial pathways induced against pathogen-associated biofilms.

CONCLUSIONS

This study confirmed the antibiofilm potential of all Schiff bases 3a-h compounds in both inhibition and eradication assays by biomass assessment. We found that the compounds generate specific results for each pathogen evaluated, with Schiff bases 3a, 3f, and 3h compounds showing the best biofilm inhibition results, while Schiff bases 3a and 3h compounds demonstrating the best biofilm eradication effects.

Further evaluation of total cell count and live/dead assays confirmed the antibiofilm properties and suggested their potential for future biomedical applications. Future studies should analyze the combination of different antibiotics with the Schiff bases 3a-h compounds to evaluate their potential synergistic effects and their eradication properties against these biofilm-forming pathogens as a therapeutic strategy. In addition, analysis of biofilm structure based on metabolic or gene expression, flow cytometry, confocal microscopy, as well as characterization of the molecular mechanisms involved in pathogens under the effect of Schiff bases will allow a better understanding of these alternative antimicrobial agents.

TABLES

Table 1. Biofilm inhibition of pathogenic microorganisms by chemical compounds.

Compound	Microorganisms	Type	Biofilm formation (%)	Biofilm inhibition (%)	Standard deviation (%)	*p*-values
3a	*S. aureus* MRSA 333	DMSO Control	91.65	8.35	7.72	0.006[a]
		Sample 10 µM	70.03	29.97	3.21	0.0000692[b]
		Sample 100 µM	71.03	28.97	6.15	0.0000696[b]
	K. pneumoniae KPC 609803	DMSO Control	76.97	23.03	9.49	0.009[a]
		Sample 10 µM	59.49	40.51	2.68	0.0000226[b]
		Sample 100 µM	60.68	39.32	3.59	0.0000484[b]
	P. aeruginosa P28	DMSO Control	98.22	1.78	5.99	0.002[a]
		Sample 10 µM	85.08	14.92	3.35	0.0000263[b]
		Sample 100 µM	86.53	13.47	7.92	0.003[b]
	E. faecalis INSPI 032	DMSO Control	93.75	6.25	7.23	0.131[a]
		Sample 10 µM	78.58	21.42	3.69	0.000149[b]
		Sample 100 µM	80.66	19.34	5.48	0.000491[b]
	C. albicans INSPI	DMSO Control	94.39	5.61	8.29	0.005[a]
		Sample 10 µM	75.88	24.12	4.71	0.004[b]
		Sample 100 µM	76.63	23.37	4.38	0.003[b]
3b	*S. aureus* MRSA 333	DMSO Control	91.65	8.35	7.72	0.006[a]
		Sample 10 µM	74.9	25.1	3.46	0.0000692[b]
		Sample 100 µM	80.05	19.95	4.6	0.000455[b]
	K. pneumoniae KPC 609803	DMSO Control	76.97	23.03	9.49	0.009[a]
		Sample 10 µM	67.83	32.17	5.38	0.005[b]
		Sample 100 µM	66.93	33.07	4.12	0.000419[b]
	P. aeruginosa P28	DMSO Control	98.22	1.78	5.99	0.002[a]
		Sample 10 µM	84.28	15.72	8.16	0.000229[b]
		Sample 100 µM	79.45	20.55	6.61	0.0000612[b]
	E. faecalis INSPI 032	DMSO Control	93.75	6.25	7.23	0.131[a]
		Sample 10 µM	80.59	19.41	5.96	0.011[b]
		Sample 100 µM	82.61	17.39	4.16	0.002[b]
	C. albicans INSPI	DMSO Control	94.39	5.61	8.29	0.00005[a]
		Sample 10 µM	63.61	36.39	8.54	0.0000269[b]
		Sample 100 µM	62.17	37.83	8.71	0.0000503[b]
3c	*S. aureus* MRSA 333	DMSO Control	91.65	8.35	7.72	0.006[a]
		Sample 10 µM	81.85	18.15	6.48	0.001[b]
		Sample 100 µM	79.48	20.52	3.35	0.000109[b]
	K. pneumoniae KPC 609803	DMSO Control	76.97	23.03	9.49	0.009[a]
		Sample 10 µM	71.22	28.78	3.93	0.125[b]
		Sample 100 µM	65.33	34.67	2.14	0.000138[b]
	P. aeruginosa P28	DMSO Control	98.22	1.78	5.99	0.002[a]
		Sample 10 µM	87.5	12.5	4.13	0.000174[b]
		Sample 100 µM	84.48	15.52	4.94	0.00012b
	E. faecalis INSPI 032	DMSO Control	93.75	6.25	7.23	0.0131[a]
		Sample 10 µM	89.46	10.54	9.88	0.311[b]
		Sample 100 µM	79.64	20.36	3.32	0.0000383[b]

	C. albicans INSPI	DMSO Control	94.39	5.61	8.29	0.005[a]
		Sample 10 µM	68.85	31.15	4.16	0.0000497[b]
		Sample 100 µM	74.18	25.82	4.9	0.000363[b]
3d	*S. aureus* MRSA 333	DMSO Control	91.65	8.35	7.72	0.006[a]
		Sample 10 µM	71.32	28.68	3.17	0.0000688[b]
		Sample 100 µM	71.74	28.26	2.93	0.0000688[b]
	K. pneumoniae KPC 609803	DMSO Control	76.97	23.03	9.49	0.009[a]
		Sample 10 µM	65.88	34.12	5.45	0.002[b]
		Sample 100 µM	62.94	37.06	7.01	0.002[b]
	P. aeruginosa P28	DMSO Control	98.22	1.78	5.99	0.002[a]
		Sample 10 µM	85.66	14.34	11.02	0.023[b]
		Sample 100 µM	85.32	14.68	12.21	0.012[b]
	E. faecalis INSPI 032	DMSO Control	93.75	6.25	7.23	0.131[a]
		Sample 10 µM	75.36	24.64	3.68	0.000017[b]
		Sample 100 µM	74.65	25.35	8.83	0.000162[b]
	C. albicans INSPI	DMSO Control	94.39	5.61	8.29	0.005[a]
		Sample 10 µM	63.52	36.48	3.81	0.0000981[b]
		Sample 100 µM	72.95	27.05	9.73	0.01[b]
3e	*S. aureus* MRSA 333	DMSO Control	91.65	8.35	7.72	0.006[a]
		Sample 10 µM	83.63	16.37	5.94	0.303[b]
		Sample 100 µM	79.21	20.79	4.69	0.0009[b]
	K. pneumoniae KPC 609803	DMSO Control	76.97	23.03	9.49	0.009[a]
		Sample 10 µM	75.13	24.87	5.74	0.798[b]
		Sample 100 µM	73.15	26.85	4.09	0.141[b]
	P. aeruginosa P28	DMSO Control	98.22	1.78	5.99	0.002[a]
		Sample 10 µM	94.45	5.55	4.45	0.083[b]
		Sample 100 µM	96.89	3.11	5.29	0.73[b]
	E. faecalis INSPI 032	DMSO Control	93.75	6.25	7.23	0.131[a]
		Sample 10 µM	84.02	15.98	8.65	0.009[b]
		Sample 100 µM	86.74	13.26	9.64	0.104[b]
	C. albicans INSPI	DMSO Control	94.39	5.61	8.29	0.005[a]
		Sample 10 µM	68.31	31.69	4.37	0.0000984[b]
		Sample 100 µM	71.45	28.55	9.12	0.003[b]
3f	*S. aureus* MRSA 333	DMSO Control	91.65	8.35	7.72	0.006[a]
		Sample 10 µM	90.67	9.33	8.46	0.952[b]
		Sample 100 µM	81.53	18.47	2.22	0.00045[b]
	K. pneumoniae KPC 609803	DMSO Control	76.97	23.03	9.49	0.009[a]
		Sample 10 µM	67.45	32.55	4.58	0.001[b]
		Sample 100 µM	72.45	27.55	2.53	0.366[b]
	P. aeruginosa P28	DMSO Control	98.22	1.78	5.99	0.002[a]
		Sample 10 µM	51.53	48.47	2.23	0.0000262[b]
		Sample 100 µM	57.69	42.31	10.2	0.0000661[b]
	E. faecalis INSPI 032	DMSO Control	93.75	6.25	7.23	0.131[a]
		Sample 10 µM	89.77	10.23	2.11	0.187[b]
		Sample 100 µM	84.46	15.54	1.66	0.003[b]
	C. albicans INSPI	DMSO Control	94.39	5.61	8.29	0.005[a]
		Sample 10 µM	63.52	36.48	3.8	0.0000981[b]
		Sample 100 µM	72.95	27.05	9.73	0.01[b]
3g		DMSO Control	91.65	8.35	7.72	0.006[a]

	S. aureus MRSA 333	Sample 10 µM	83.46	16.54	6.82	0.045[b]
		Sample 100 µM	88.52	11.48	9.72	0.251[b]
	K. pneumoniae KPC 609803	DMSO Control	76.97	23.03	9.49	0.009[a]
		Sample 10 µM	70.31	29.69	3.34	0.03[b]
		Sample 100 µM	70.83	29.17	6.4	0.04[b]
	P. aeruginosa P28	DMSO Control	98.22	1.78	5.99	0.002[a]
		Sample 10 µM	89.98	10.02	7.15	0.006[b]
		Sample 100 µM	99.44	0.56	5.66	0.396[b]
	E. faecalis INSPI 032	DMSO Control	93.75	6.25	7.23	0.131[a]
		Sample 10 µM	82.51	17.49	3.33	0.01b
		Sample 100 µM	83.69	16.31	4.35	0.00096[b]
	C. albicans INSPI	DMSO Control	94.39	5.61	8.29	0.005[a]
		Sample 10 µM	69.34	30.66	3.94	0.0005[b]
		Sample 100 µM	71.16	28.84	2.53	0.0005[b]
3h	*S. aureus* MRSA 333	DMSO Control	91.65	8.35	7.72	0.006[a]
		Sample 10 µM	73.32	26.68	3.53	0.0000337[b]
		Sample 100 µM	72.81	27.19	4.13	0.0000337[b]
	K. pneumoniae KPC 609803	DMSO Control	76.97	23.03	9.49	0.009[a]
		Sample 10 µM	70.68	29.32	3.82	0.07[b]
		Sample 100 µM	71.06	28.94	5.38	0.254[b]
	P. aeruginosa P28	DMSO Control	98.22	1.78	5.99	0.002[a]
		Sample 10 µM	83.55	16.45	2.67	0.000011[b]
		Sample 100 µM	88.71	11.29	6.36	0.006[b]
	E. faecalis INSPI 032	DMSO Control	93.75	6.25	7.23	0.131[a]
		Sample 10 µM	77.37	22.63	3.82	0.002[b]
		Sample 100 µM	79.43	20.57	4.11	0.0000125[b]
	C. albicans INSPI	DMSO Control	94.39	5.61	8.29	0.005[a]
		Sample 10 µM	72.35	27.65	5.15	0.000156[b]
		Sample 100 µM	71.03	28.97	2.38	0.0000497[b]

Legend: Evaluated concentrations of the present study are indicated in each compound information. Biofilm formation values of DMSO 100% controls and samples were calculated as the percentage of pathogen biofilm formation through the optical density comparison between DMSO controls/samples and pathogen growth in only medium culture (positive control). The experimental positive controls were considered as 100.00% when compared to the DMSO control and samples in the assays. All negative controls of the pathogens showed no growth of the pathogen in 96-well plates, being considered as 0.00% after the deduction of the optical density of the medium culture in all controls and samples in the biofilm assays. All statistical analyses (*p*-values) were analyzed using a non-parametric Wilcoxon test (95% confidence interval) for comparison between biofilm formation values. [a] *p*-values obtained when comparing positive controls and DMSO controls. [b] *p*-values obtained when comparing DMSO controls and samples.

Table 2. Biofilm eradication of pathogenic microorganisms by chemical compounds**.**

Compound	Microorganisms	Type	Biofilm formation (%)	Biofilm eradication (%)	Standard deviation (%)	p-values
3a	*S. aureus* MRSA 333	DMSO Control	99.45	0.55	5.37	0.915[a]
		Sample 10 µM	90.56	9.44	4.86	0.141[b]
		Sample 100 µM	84.81	15.19	7.96	0.0000496[b]
	K. pneumoniae KPC 609803	DMSO Control	83.58	16.42	5.34	0.000067[a]
		Sample 10 µM	84.87	15.13	5.22	0.412[b]
		Sample 100 µM	82.07	17.93	5.54	0.383[b]
	P. aeruginosa P28	DMSO Control	81.26	18.74	0.83	0.0000198[a]
		Sample 10 µM	70.75	29.25	1.81	0.0000432[b]
		Sample 100 µM	70.14	29.86	3.16	0.0000431[b]
	E. faecalis INSPI 032	DMSO Control	93.05	6.95	7.29	0.102[a]
		Sample 10 µM	80.85	19.15	5.40	0.001[b]
		Sample 100 µM	79.90	20.10	4.79	0.000392[b]
	C. albicans INSPI	DMSO Control	100.23	-0.23	8.35	0.825[a]
		Sample 10 µM	71.17	28.83	6.34	0.000185[b]
		Sample 100 µM	75.60	24.40	3.30	0.000184[b]
3b	*S. aureus* MRSA 333	DMSO Control	99.45	0.55	5.37	0.915[a]
		Sample 10 µM	95.72	4.28	2.82	0.105[b]
		Sample 100 µM	89.56	10.44	4.76	0.001[b]
	K. pneumoniae KPC 609803	DMSO Control	83.58	16.42	5.34	0.000067[a]
		Sample 10 µM	79.93	20.07	5.57	0.507[b]
		Sample 100 µM	79.44	20.56	5.17	0.12[b]
	P. aeruginosa P28	DMSO Control	81.26	18.74	0.83	0.0000198[a]
		Sample 10 µM	79.25	20.75	5.26	0.315[b]
		Sample 100 µM	78.95	21.05	8.26	0.573[b]
	E. faecalis INSPI 032	DMSO Control	93.05	6.95	7.29	0.102[a]
		Sample 10 µM	82.34	17.66	7.03	0.001[b]
		Sample 100 µM	79.08	20.92	4.25	0.000436[b]
	C. albicans INSPI	DMSO Control	100.23	-0.23	8.35	0.825[a]
		Sample 10 µM	75.32	24.68	4.34	0.000353[b]
		Sample 100 µM	74.01	25.99	4.90	0.000355[b]
3c	*S. aureus* MRSA 333	DMSO Control	99.45	0.55	5.37	0.915[a]
		Sample 10 µM	86.10	13.90	5.37	0.000759[b]
		Sample 100 µM	84.29	15.71	5.70	0.0000679[b]
	K. pneumoniae KPC 609803	DMSO Control	83.58	16.42	5.34	0.000067[a]
		Sample 10 µM	82.57	17.43	3.05	0.891[b]
		Sample 100 µM	82.24	17.76	4.28	0.583[b]
	P. aeruginosa P28	DMSO Control	81.26	18.74	0.83	0.0000198[a]
		Sample 10 µM	75.15	24.85	8.40	0.032[b]
		Sample 100 µM	75.61	24.39	6.01	0.023[b]
	E. faecalis INSPI 032	DMSO Control	93.05	6.95	7.29	0.102[a]
		Sample 10 µM	81.01	18.99	3.71	0.0000935[b]
		Sample 100 µM	76.65	23.35	2.83	0.00034[b]
		DMSO Control	100.23	-0.23	8.35	0.825[a]

	C. albicans INSPI	Sample 10 µM	82.46	17.54	8.78	0.002[b]
		Sample 100 µM	83.13	16.87	6.02	0.000178[b]
3d	*S. aureus* MRSA 333	DMSO Control	99.45	0.55	5.37	0.915[a]
		Sample 10 µM	84.23	15.77	7.15	0.000276[b]
		Sample 100 µM	85.67	14.33	3.09	0.000113[b]
	K. pneumoniae KPC 609803	DMSO Control	83.58	16.42	5.34	0.000067[a]
		Sample 10 µM	76.61	23.39	3.00	0.000239[b]
		Sample 100 µM	77.49	22.51	3.12	0.0009320[b]
	P. aeruginosa P28	DMSO Control	81.26	18.74	0.83	0.0000198[a]
		Sample 10 µM	77.13	22.87	4.81	0.026[b]
		Sample 100 µM	79.10	20.90	7.88	0.331[b]
	E. faecalis INSPI 032	DMSO Control	93.05	6.95	7.29	0.102[a]
		Sample 10 µM	85.49	14.51	4.80	0.008[b]
		Sample 100 µM	86.81	13.19	3.34	0.035[b]
	C. albicans INSPI	DMSO Control	100.23	-0.23	8.35	0.825[a]
		Sample 10 µM	89.78	10.22	11.18	0.042[b]
		Sample 100 µM	89.63	10.37	9.64	0.059[b]
3e	*S. aureus* MRSA 333	DMSO Control	99.45	0.55	5.37	0.915[a]
		Sample 10 µM	83.05	16.95	6.30	0.000112[b]
		Sample 100 µM	81.65	18.35	2.13	0.0000491[b]
	K. pneumoniae KPC 609803	DMSO Control	83.58	16.42	5.34	0.000067[a]
		Sample 10 µM	79.09	20.91	4.53	0.024[b]
		Sample 100 µM	78.22	21.78	2.80	0.004[b]
	P. aeruginosa P28	DMSO Control	81.26	18.74	0.83	0.0000198[a]
		Sample 10 µM	84.26	15.74	7.71	0.344[b]
		Sample 100 µM	72.57	27.43	5.76	0.000906[b]
	E. faecalis INSPI 032	DMSO Control	93.05	6.95	7.29	0.102[a]
		Sample 10 µM	85.77	14.23	4.64	0.006[b]
		Sample 100 µM	83.72	16.28	3.88	0.001[b]
	C. albicans INSPI	DMSO Control	100.23	-0.23	8.35	0.825[a]
		Sample 10 µM	96.64	3.36	3.40	0.428[b]
		Sample 100 µM	89.03	10.97	9.44	0.019[b]
3f	*S. aureus* MRSA 333	DMSO Control	99.45	0.55	5.37	0.915[a]
		Sample 10 µM	79.03	20.97	2.22	0.000113[b]
		Sample 100 µM	77.77	22.23	1.64	0.0000483[b]
	K. pneumoniae KPC 609803	DMSO Control	83.58	16.42	5.34	0.000067[a]
		Sample 10 µM	84.65	15.35	5.39	0.197[b]
		Sample 100 µM	75.82	24.18	6.29	0.013[b]
	P. aeruginosa P28	DMSO Control	81.26	18.74	0.83	0.0000198[a]
		Sample 10 µM	81.68	18.32	5.87	0.4430[b]
		Sample 100 µM	84.11	15.89	8.21	0.778[b]
	E. faecalis INSPI 032	DMSO Control	93.05	6.95	7.29	0.102[a]
		Sample 10 µM	87.28	12.72	6.56	0.107[b]
		Sample 100 µM	91.12	8.88	4.76	0.440[b]
	C. albicans INSPI	DMSO Control	100.23	-0.23	8.35	0.825[a]
		Sample 10 µM	83.89	16.11	4.69	0.002[b]
		Sample 100 µM	82.67	17.33	1.64	0.000184[b]
3g		DMSO Control	99.45	0.55	5.37	0.915[a]

	S. aureus MRSA 333	Sample 10 µM	86.87	13.13	4.20	0.000513[b]
		Sample 100 µM	79.77	20.23	5.01	0.000276[b]
	K. pneumoniae KPC 609803	DMSO Control	83.58	16.42	5.34	0.000067[a]
		Sample 10 µM	75.66	24.34	7.34	0.002[b]
		Sample 100 µM	73.83	26.17	6.08	0.002[b]
	P. aeruginosa P28	DMSO Control	81.26	18.74	0.83	0.0000198[a]
		Sample 10 µM	76.21	23.79	7.76	0.09[b]
		Sample 100 µM	70.75	29.25	2.89	0.0000494[b]
	E. faecalis INSPI 032	DMSO Control	93.05	6.95	7.29	0.102[a]
		Sample 10 µM	82.55	17.45	4.44	0.000597[b]
		Sample 100 µM	80.85	19.15	5.10	0.000484[b]
	C. albicans INSPI	DMSO Control	100.23	-0.23	8.35	0.825[a]
		Sample 10 µM	74.62	25.38	3.96	0.000188[b]
		Sample 100 µM	77.76	22.24	1.77	0.000353[b]
3h	*S. aureus* MRSA 333	DMSO Control	99.45	0.55	5.37	0.915[a]
		Sample 10 µM	75.81	24.19	2.98	0.000113[b]
		Sample 100 µM	76.48	23.52	2.77	0.000275[b]
	K. pneumoniae KPC 609803	DMSO Control	83.58	16.42	5.34	0.000067[a]
		Sample 10 µM	69.55	30.45	3.35	0.0000765[b]
		Sample 100 µM	68.09	31.91	2.08	0.0000316[b]
	P. aeruginosa P28	DMSO Control	81.26	18.74	0.83	0.0000231[a]
		Sample 10 µM	81.53	18.47	5.68	0.980000[b]
		Sample 100 µM	76.67	23.33	7.56	0.015[b]
	E. faecalis INSPI 032	DMSO Control	93.05	6.95	7.29	0.102[a]
		Sample 10 µM	78.73	21.27	4.25	0.000856[b]
		Sample 100 µM	78.57	21.43	2.83	0.000145[b]
	C. albicans INSPI	DMSO Control	100.23	-0.23	8.35	0.825[a]
		Sample 10 µM	77.43	22.57	3.44	0.000104[b]
		Sample 100 µM	77.95	22.05	3.70	0.000355[b]

Legend: Evaluated concentrations of the present study are indicated in each compound information. Biofilm formation values of DMSO 100% controls and samples were calculated as the percentage of pathogen biofilm formation through the optical density comparison between DMSO controls/samples and pathogen growth in only medium culture (positive control). The experimental positive controls were considered as 100.00% when compared to the DMSO control and samples in the assays. All negative controls of the pathogens showed no growth of the pathogen in 96-well plates. being considered as 0.00% after the deduction of the optical density of the medium culture in all controls and samples in the biofilm assays. All statistical analyses (*p*-values) were analyzed using a non-parametric Wilcoxon test (95% confidence interval) for comparison between biofilm formation values. [a] *p*-values obtained when comparing positive controls and DMSO controls. [b] *p*-values obtained when comparing DMSO controls and samples.

Table 3. The overall results obtained by epifluorescence microscopy with LIVE/DEAD staining assays from Microscopy Analysis**.**

Epifluorescence microscopy (EM) with LIVE/DEAD Staining

	***P. aeruginosa* P28 Schiff base f compound**						***C. albicans* INSPI Schiff base f compound**					
Assay	**Mean of cells/frame (SD)[c]**	**Mean of cells/cm² (SD) [d]**	**Dead (SD) %**	**Live (SD) %**	**Wilcoxon [a] test *p*-value**	**Wilcoxon [b] test *p*-value**	**Mean of cells/frame (SD)**	**Mean of cells/cm² (SD) [d]**	**Dead (SD) %**	**Live (SD) %**	**Wilcoxon [a] test *p*-value**	**Wilcoxon [b] test *p*-value**
C+	1729.57	13428312.63	11.07	89.22			415.93	3229270.19	6.45	93.55		
	0.16	0.16	0.04	0.02			30.31	30.31	2.79	0.19		
DMSO	1725.99	13400515.25	92.61	7.39	5.26E-01	1.63e-08	23.99	186257.76	21.16	78.84	9.44e-09	5.90E-02
	0.05	0.05	0.03	12.59			10.97	85170.81	3.75	1.01		
10 μM	842.41	6540467.41	78.61	21.39	6.26E-01	6.23e-01	8.18	63509.32	36.85	63.15	1.63e-05	2.50E-01
	0.18	0.18	1.47	4.83			35.13	272748.45	2.00	1.17		
100 μM	1313.86	10200777.32	94.72	5.28	1.58E-01	2.00e-03	8.01	62158.39	40.02	59.98	5.83e-06	2.01E-01
	0.06	0.06	0.97	17.38			10.20	10.20	1.49	0.99		

	***K. pneumoniae* KPC 609803 Schiff base a compound**						***S. aureus* MRSA 333 Schiff base a compound**						***E. faecalis* INSPI 032 Schiff base d compound**					
Assay	**Mean of cells/frame (SD)[c]**	**Mean of cells/cm² (SD) [d]**	**Dead (SD) %**	**Live (SD) %**	**Wilcoxon [a] test *p*-value**	**Wilcoxon [b] test *p*-value**	**Mean of cells/frame (SD)**	**Mean of cells/cm² (SD) [d]**	**Dead (SD) %**	**Live (SD) %**	**Wilcoxon [a] test *p*-value**	**Wilcoxon [b] test *p*-value**	**Mean of cells/frame (SD)**	**Mean of cells/cm² (SD) [d]**	**Dead (SD) %**	**Live (SD) %**	**Wilcoxon [a] test *p*-value**	**Wilcoxon [b] test *p*-value**
C+	467.02	3625952.85	30.70	69.30			1396.86	10845164.15	32.17	67.83			1035.46	8039285.71	15.25	84.75		
	0.16	0.16	1.10	8.60			0.28	0.28	0.17	0.08			15.25	15.25	7.45	1.34		
DMSO	287.51	2232250.69	42.90	57.10	8.00E-01	7.45e-07	1268.76	9850598.94	67.29	32.71	4.7e-01	4.85e-04	464.61	3607220.50	36.80	63.20	1.45e-08	4.00E-03
	0.45	0.45	3.40	4.80			0.41	0.41	1.03	2.13			36.80	36.80	4.28	2.49		
100 μM	427.77	3321194.42	94.60	5.40	1.47E-07	3.26e-01	1348.86	10472533.96	89.92	10.08	3.31e-06	5.89e-08	687.26	5335869.57	31.89	68.11	1.90e-01	2.23E-01
	0.13	0.13	1.60	10.40			0.14	0.14	0.83	7.45			31.89	31.89	3.84	1.80		

Legend: Results obtained from fluorescence microscopy analysis. The best Schiff bases compound for each species was selected to compare the biofilm structure between treated and non-treated biofilm samples by live/dead staining assay using epifluorescence microscopy. The number of total cells and live/dead cells were quantified through ImageJ by Fiji version 1.57 using the macros Biofilms Viability checker (see methods). Images were processed by a sequence of modules forming a pipeline in Cell Profiler software. The pipeline is described and can be revised in the supplemental material. DAPI images were used to obtain the total cells per image. [a] Wilcoxon test was realized in the number of total cells by compared with DMSO control. [b] Wilcoxon test was realized in the number of dead cells compared with DMSO control. In each assay. we collected at least 15 photographs for counting. [c] Average of photographs and SD. [d] microorganism/cm^2 obtain by formula: average of cells (SD)* (1E+08/12880).

FIGURES.

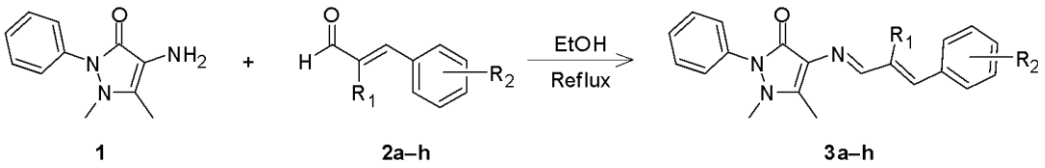

1 2a–h 3a–h

	R_1	R_2
3a	H	H
3b	H	2-NO_2
3c	H	2-OMe
3d	H	4-NMe_2
3e	H	3-OMe-4-OAc
3f	Br	H
3g	Me	H
3h	H	4-NO_2

Figure 1. A general illustration of the studied Schiff bases 3a–h compounds.

Legend: The figure shows the synthesis reaction of the base structure for the Schiff bases, the radioacles named R1 and R2, will change with the functional groups listed in points 3a to 3h. 3a has in its radicals a hydrogen group, 3b in radical 1 hydrogen in radical two, nitrogen dioxide in carbon 2, compound 3c has in the first radical hydrogen, and radical 2 an oxymethylene ether located in carbon 2. 3d hydrogen in its first radical and tetrakis in radical two in carbon 4. Compound 3e contains hydrogen and oxymethylene ether at carbon 3 and palladium acetate at carbon 4. 3f and 3 g have hydrogen in their second radical while in the first radical bromine and methyl respectively. Finally, compound 3h contains hydrogen at its first radical and nitrogen dioxide at carbon 4 of its second radical.

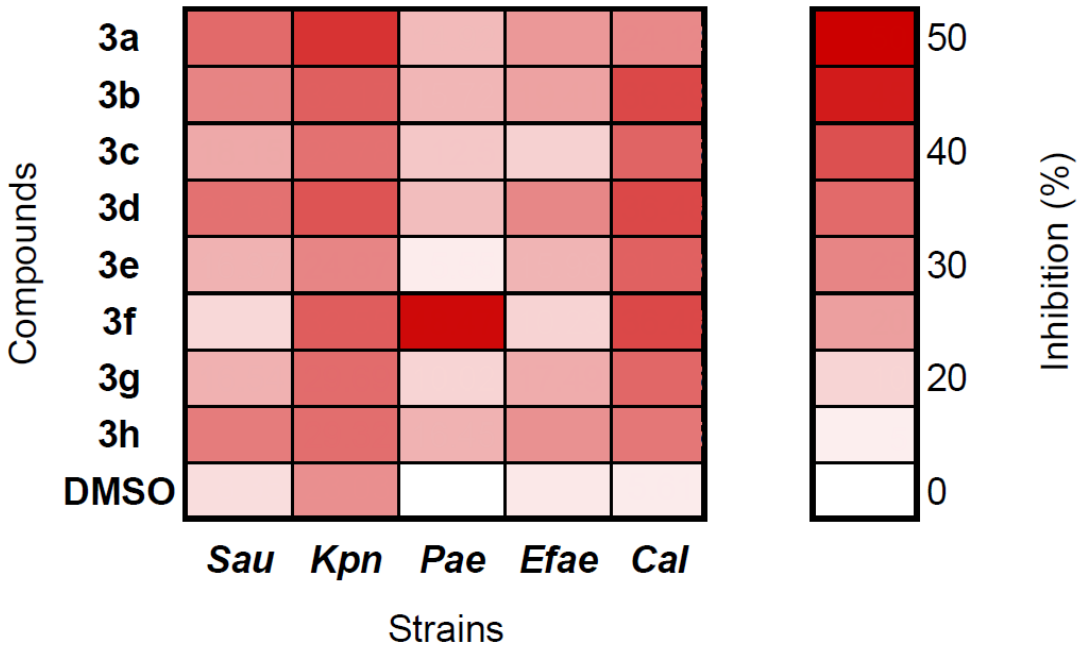

Figure 2. Illustrative representation of the main results obtained in the biofilm inhibition assays.

Legend: The five biofilm-producing microorganisms, more exactly, *Staphylococcus aureus* (Sau), *Klebsiella pneumoniae* (Kpn), *Pseudomonas aeruginosa* (Pae), *Enterococcus faecalis* (Efa), and *Candida albicans* (Cal), were incubated for 24 hours at 37°C in bottom flat 96-well plates with 10 µM of each of the Schiff bases (3a-3h compounds). The inhibition values detailed in Table 1 and presented in this figure as shades of red, correspond to the average of the difference between the production of each microorganism in the absence of the compounds and counteracted the effect of the solvent used (DMSO) on the biofilm inhibition of each microorganism.

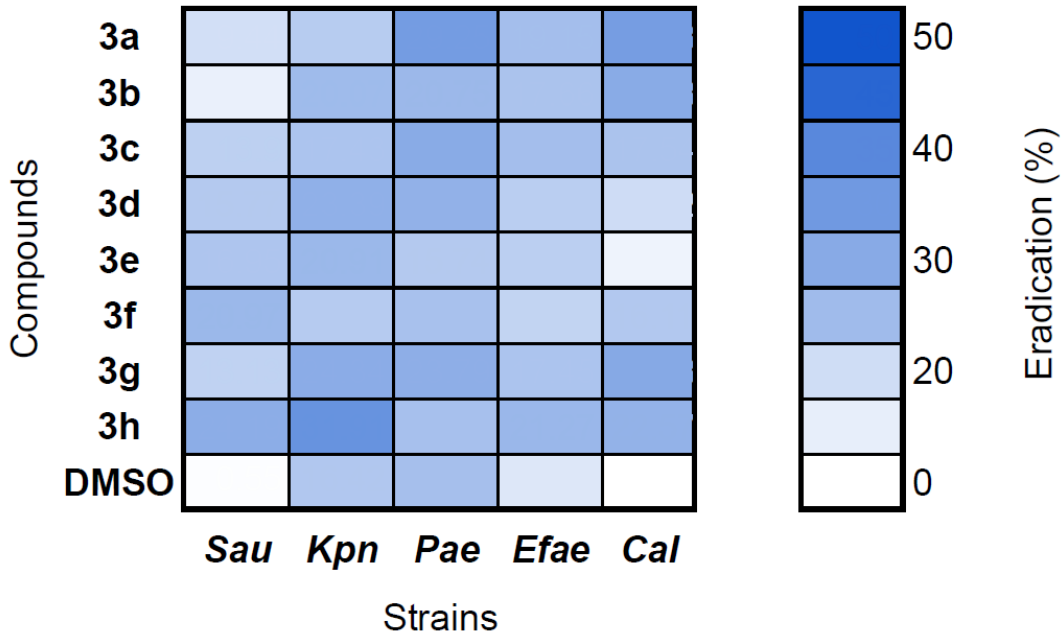

Figure 3. Illustrative representation of the main results obtained in the biofilm eradication assays.

Legend: The five biofilm-producing microorganisms, more exactly, *Staphylococcus aureus* (Sau), *Klebsiella pneumoniae* (Kpn), *Pseudomonas aeruginosa* (Pae), *Enterococcus faecalis* (Efa), and *Candida albicans* (Cal), were incubated for 24 hours at 37°C in bottom flat 96-well plates without any additions to allow the production of biofilm. After this point, 10 µM of each Schiff base (3a-3h compounds) was added to each well and plates were incubated at 37 for another 24 hours. The eradication values detailed in Table 2 and presented in this figure as shades of blue, correspond to the average of the difference between the persistent biofilm of each microorganism in the absence of the compounds and counteracted the effect of the solvent used (DMSO) on the biofilm eradication of each microorganism.

REFERENCES

Amer, H. H., Eldrehmy, E. H., Abdel-Hafez, S. M., Alghamdi, Y. S., Hassan, M. Y., & Alotaibi, S. H. (2021). Antibacterial and molecular docking studies of newly synthesized nucleosides and Schiff bases derived from sulfadimidines. *Scientific Reports*, *11*(1). https://doi.org/10.1038/s41598-021-97297-1

Arshia, Khan, A. K., Khan, K. M., Ahmed, A., Taha, M., & Perveen, S. (2017). Antibiofilm potential of synthetic 2-amino-5-chlorobenzophenone Schiff bases and its confirmation through fluorescence microscopy. *Microbial Pathogenesis*, *110*. https://doi.org/10.1016/j.micpath.2017.07.040

Atiencia-Carrera, M. B., Cabezas-Mera, F. S., Tejera, E., & Machado, A. (2022). Prevalence of biofilms in Candida spp. bloodstream infections: a meta-analysis. *PLoS ONE*, *17*(2), e0263522. https://doi.org/10.1371/journal.pone.0263522

Atiencia-Carrera, M. B., Cabezas-Mera, F. S., Vizuete, K., Debut, A., Tejera, E., & Machado, A. (2022). Evaluation of the biofilm life cycle between Candida albicans and Candida tropicalis. *Front. Cell. Infect. Microbiol.*, *12*, 953168. https://doi.org/10.3389/fcimb.2022.953168

Biswas, S., Wasai, A., Ghosh, M., Rizzoli, C., Roy, A., Saha, S., & Mandal, S. (2023). A mononuclear N,N,N,O donor schiff base Cu(II) complex inhibits bacterial biofilm formation and promotes apoptosis and cell cycle arrest in prostate cancer cells. *Journal of Inorganic Biochemistry*, *247*. https://doi.org/10.1016/j.jinorgbio.2023.112314

Cabezas-Mera, F. S., Atiencia-Carrera, M. B., Villacrés-Granda, I., Proaño, A. A., Debut, A., Vizuete, K., Herrero-Bayo, L., Gonzalez-Paramás, A. M., Giampieri, F., Abreu-Naranjo, R., Tejera, E., Álvarez-Suarez, J. M., & Machado, A. (2023). Evaluation of the polyphenolic profile of native Ecuadorian stingless bee honeys (Tribe: Meliponini) and their antibiofilm activity on susceptible and multidrug-resistant pathogens: An exploratory analysis. *Current Research in Food Science*, *7*, 100543. https://doi.org/10.1016/j.crfs.2023.100543

Cangui-Panchi, S. P., Ñacato-Toapanta, A. L., Enríquez-Martínez, L. J., Reyes, J., Garzon-Chavez, D., & Machado, A. (2022). Biofilm-forming microorganisms causing hospital-acquired infections from intravenous catheter: A systematic review. *Current Research in Microbial Sciences*, *3*. https://doi.org/10.1016/j.crmicr.2022.100175

Cangui-Panchi, S. P., Ñacato-Toapanta, A. L., Enríquez-Martínez, L. J., Salinas-Delgado, G. A., Reyes, J., Garzon-Chavez, D., & Machado, A. (2023). Battle royale: Immune response on biofilms – host-pathogen interactions. *Current Research in Immunology*, *4*(March). https://doi.org/10.1016/j.crimmu.2023.100057

Ceramella, J., Iacopetta, D., Catalano, A., Cirillo, F., Lappano, R., & Sinicropi, M. S. (2022). A Review on the Antimicrobial Activity of Schiff Bases: Data Collection and Recent Studies. In *Antibiotics* (Vol. 11, Issue 2). https://doi.org/10.3390/antibiotics11020191

Chinemerem Nwobodo, D., Ugwu, M. C., Oliseloke Anie, C., Al-Ouqaili, M. T. S., Chinedu Ikem, J., Victor Chigozie, U., & Saki, M. (2022). Antibiotic resistance: The challenges and some emerging strategies for tackling a global menace. In *Journal of Clinical Laboratory Analysis* (Vol. 36, Issue 9). https://doi.org/10.1002/jcla.24655

Chung, P. Y., Khoo, R. E. Y., Liew, H. S., & Low, M. L. (2021). Antimicrobial and antibiofilm activities of Cu(II) Schiff base complexes against methicillin-susceptible

and resistant Staphylococcus aureus. *Annals of Clinical Microbiology and Antimicrobials*, *20*(1). https://doi.org/10.1186/s12941-021-00473-4

Conected Pappers. (n.d.). *Biofilm reports*.

Da Silva, C. M., Da Silva, D. L., Modolo, L. V., Alves, R. B., De Resende, M. A., Martins, C. V. B., & De Fátima, Â. (2011). Schiff bases: A short review of their antimicrobial activities. In *Journal of Advanced Research* (Vol. 2, Issue 1). https://doi.org/10.1016/j.jare.2010.05.004

Elmehbad, N. Y., Mohamed, N. A., & Abd El-Ghany, N. A. (2022). Evaluation of the antimicrobial and anti-biofilm activity of novel salicylhydrazido chitosan derivatives impregnated with titanium dioxide nanoparticles. *International Journal of Biological Macromolecules*, *205*. https://doi.org/10.1016/j.ijbiomac.2022.03.076

Fernandez-Soto, P., Celi, D., Tejera, E., Alvarez-Suarez, J. M., & Machado, A. (2023). Cinnamomum sp. and Pelargonium odoratissimum as the Main Contributors to the Antibacterial Activity of the Medicinal Drink Horchata: A Study Based on the Antibacterial and Chemical Analysis of 21 Plants. *Molecules*, *28*(2), 693. https://doi.org/10.3390/molecules28020693

Gulati, M., & Nobile, C. J. (2016). Candida albicans biofilms: development, regulation, and molecular mechanisms. In *Microbes and Infection* (Vol. 18, Issue 5). https://doi.org/10.1016/j.micinf.2016.01.002

Kassambara, A. (2021). Pipe-friendly framework for basic statistical tests [R Package "rstatix" version 0.7. 0]. In *R Foundation for Statistical Computing, Vienna*.

Kwon, J. H., & Powderly, W. G. (2021). The post-antibiotic era is here. *Science*, *373*(6554), 471. https://doi.org/10.1126/science.abl5997

Machado, A., Zamora-Mendoza, L., Alexis, F., & Álvarez-Suarez, J. M. (2023a). Use of Plant Extracts, Bee-Derived Products, and Probiotic-Related Applications to Fight Multidrug-Resistant Pathogens in the Post-Antibiotic Era. *Future Pharmacology*, *3*(3). https://doi.org/10.3390/futurepharmacol3030034

Machado, A., Zamora-Mendoza, L., Alexis, F., & Álvarez-Suarez, J. M. (2023b). Use of Plant Extracts, Bee-Derived Products, and Probiotic-Related Applications to Fight Multidrug-Resistant Pathogens in the Post-Antibiotic Era. *Future Pharmacology*, *3*(3), 535–567. https://doi.org/10.3390/futurepharmacol3030034

Mastoor, S., Nazim, F., Rizwan-ul-Hasan, S., Ahmed, K., Khan, S., Ali, S. N., & Abidi, S. H. (2022). Analysis of the Antimicrobial and Anti-Biofilm Activity of Natural Compounds and Their Analogues against Staphylococcus aureus Isolates. *Molecules*, *27*(20). https://doi.org/10.3390/molecules27206874

Mohini, Y., Prasad, R. B. N., Karuna, M. S. L., Poornachandra, Y., & Ganesh Kumar, C. (2014). Synthesis, antimicrobial and anti-biofilm activities of novel Schiff base analogues derived from methyl-12-aminooctadec-9-enoate. *Bioorganic and Medicinal Chemistry Letters*, *24*(22). https://doi.org/10.1016/j.bmcl.2014.09.062

More, P. G., Karale, N. N., Lawand, A. S., Narang, N., & Patil, R. H. (2013). Synthesis and anti-biofilm activity of thiazole Schiff bases. *Medicinal Chemistry Research*, *23*(2), 790–799. https://doi.org/10.1007/s00044-013-0672-7

Mountcastle, S. E., Vyas, N., Villapun, V. M., Cox, S. C., Jabbari, S., Sammons, R. L., Shelton, R. M., Walmsley, A. D., & Kuehne, S. A. (2021). Biofilm viability checker: An open-source tool for automated biofilm viability analysis from confocal microscopy images. *Npj Biofilms and Microbiomes*, *7*(1). https://doi.org/10.1038/s41522-021-00214-7

Murray, C. J., Ikuta, K. S., Sharara, F., Swetschinski, L., Robles Aguilar, G., Gray, A., Han, C., Bisignano, C., Rao, P., Wool, E., Johnson, S. C., Browne, A. J., Chipeta,

M. G., Fell, F., Hackett, S., Haines-Woodhouse, G., Kashef Hamadani, B. H., Kumaran, E. A. P., McManigal, B., … Naghavi, M. (2022). Global burden of bacterial antimicrobial resistance in 2019: a systematic analysis. *The Lancet*, *399*(10325). https://doi.org/10.1016/S0140-6736(21)02724-0

Patel, M., Siddiqui, A. J., Hamadou, W. S., Surti, M., Awadelkareem, A. M., Ashraf, S. A., Alreshidi, M., Snoussi, M., Rizvi, S. M. D., Bardakci, F., Jamal, A., Sachidanandan, M., & Adnan, M. (2021). Inhibition of bacterial adhesion and antibiofilm activities of a glycolipid biosurfactant from lactobacillus rhamnosus with its physicochemical and functional properties. *Antibiotics*, *10*(12). https://doi.org/10.3390/antibiotics10121546

Rakhmawatie, M. D., Wibawa, T., Lisdiyanti, P., Pratiwi, W. R., & Mustofa. (2019). Evaluation of crystal violet decolorization assay and resazurin microplate assay for antimycobacterial screening. *Heliyon*, *5*(8). https://doi.org/10.1016/j.heliyon.2019.e02263

Reardon, S. (2014). WHO warns against "post-antibiotic" era. *Nature*, *April*, 1–2. https://doi.org/10.1038/nature.2014.15135

Rosenberg, M., Azevedo, N. F., & Ivask, A. (2019). Propidium iodide staining underestimates viability of adherent bacterial cells. *Scientific Reports*, *9*(1). https://doi.org/10.1038/s41598-019-42906-3

Salam, M. A., Al-Amin, M. Y., Salam, M. T., Pawar, J. S., Akhter, N., Rabaan, A. A., & Alqumber, M. A. A. (2023). Antimicrobial Resistance: A Growing Serious Threat for Global Public Health. In *Healthcare (Switzerland)* (Vol. 11, Issue 13). https://doi.org/10.3390/healthcare11131946

Schindelin, J., Arganda-Carreras, I., Frise, E., Kaynig, V., Longair, M., Pietzsch, T., Preibisch, S., Rueden, C., Saalfeld, S., Schmid, B., Tinevez, J. Y., White, D. J., Hartenstein, V., Eliceiri, K., Tomancak, P., & Cardona, A. (2012). Fiji: An open-source platform for biological-image analysis. In *Nature Methods* (Vol. 9, Issue 7). https://doi.org/10.1038/nmeth.2019

Sharma, D., Misba, L., & Khan, A. U. (2019). Antibiotics versus biofilm: An emerging battleground in microbial communities. In *Antimicrobial Resistance and Infection Control* (Vol. 8, Issue 1). https://doi.org/10.1186/s13756-019-0533-3

Silva, V., Almeida, L., Gaio, V., Cerca, N., Manageiro, V., Caniça, M., Capelo, J. L., Igrejas, G., & Poeta, P. (2021). Biofilm formation of multidrug-resistant mrsa strains isolated from different types of human infections. *Pathogens*, *10*(8). https://doi.org/10.3390/pathogens10080970

Sindelo, A., Sen, P., & Nyokong, T. (2023). Photoantimicrobial activity of Schiff-base morpholino phthalocyanines against drug resistant micro-organisms in their planktonic and biofilm forms. *Photodiagnosis and Photodynamic Therapy*, *42*. https://doi.org/10.1016/j.pdpdt.2023.103519

Sornsenee, P., Chatatikun, M., Mitsuwan, W., Kongpol, K., Kooltheat, N., Sohbenalee, S., Pruksaphanrat, S., Mudpan, A., & Romyasamit, C. (2021). Lyophilized cell-free supernatants of Lactobacillus isolates exhibited antibiofilm, antioxidant, and reduces nitric oxide activity in lipopolysaccharide- stimulated RAW 264.7 cells. *PeerJ*, *9*. https://doi.org/10.7717/peerj.12586

Srinivasan, V., Khamrang, T., Ponraj, C., Saravanan, D., Yamini, R., Bera, S., & Jhonsi, M. A. (2021). Pyrene based Schiff bases: Synthesis, crystal structure, antibacterial and BSA binding studies. *Journal of Molecular Structure*, *1225*. https://doi.org/10.1016/j.molstruc.2020.129153

Stolarczyk, M., Wolska, A., Mikołajczyk, A., Bryndal, I., Cieplik, J., Lis, T., & Matera-Witkiewicz, A. (2021). A new pyrimidine schiff base with selective activities against enterococcus faecalis and gastric adenocarcinoma. *Molecules*, *26*(8). https://doi.org/10.3390/molecules26082296

Teran, Guevara, Mora, Dobronski, Barreiro-Costa, Beske, Pérez-Barrera, Araya-Maturana, Rojas-Silva, Poveda, & Heredia-Moya. (2019). Characterization of Antimicrobial, Antioxidant, and Leishmanicidal Activities of Schiff Base Derivatives of 4-Aminoantipyrine. *Molecules*, *24*(15), 2696. https://doi.org/10.3390/molecules24152696

Tsacheva, I., Todorova, Z., Momekova, D., Momekov, G., & Koseva, N. (2023). Pharmacological Activities of Schiff Bases and Their Derivatives with Low and High Molecular Phosphonates. In *Pharmaceuticals* (Vol. 16, Issue 7). https://doi.org/10.3390/ph16070938

Tuna Subasi, N. (2023). Overview of Schiff Bases. In *Schiff Base in Organic, Inorganic and Physical Chemistry*. https://doi.org/10.5772/intechopen.108178

Vani, S., Vadakkan, K., & Mani, B. (2023). A narrative review on bacterial biofilm: its formation, clinical aspects and inhibition strategies. *Future Journal of Pharmaceutical Sciences*, *9*(1). https://doi.org/10.1186/s43094-023-00499-9

Wickham, H., Averick, M., Bryan, J., Chang, W., McGowan, L., François, R., Grolemund, G., Hayes, A., Henry, L., Hester, J., Kuhn, M., Pedersen, T., Miller, E., Bache, S., Müller, K., Ooms, J., Robinson, D., Seidel, D., Spinu, V., … Yutani, H. (2019). Welcome to the Tidyverse. *Journal of Open Source Software*, *4*(43). https://doi.org/10.21105/joss.01686

APPENDIX

APPENDIX 1: DEATHS ATTRIBUTABLE TO AND ASSOCIATED WITH BACTERIAL ANTIMICROBIAL RESISTANCE BY GBD REGION, DURING 2019.

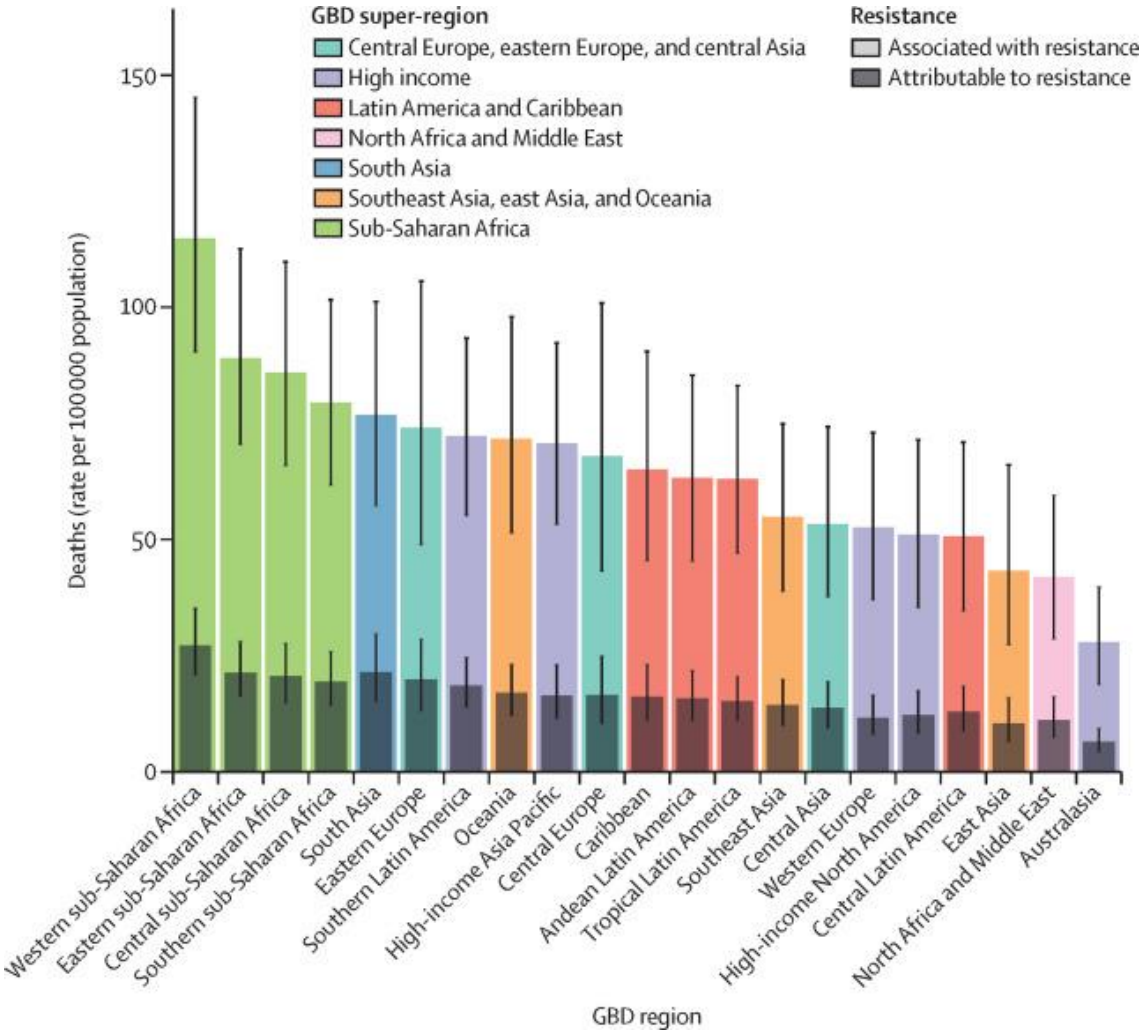

All-age rate of deaths attributable to and associated with bacterial antimicrobial resistance by GBD region, 2019. Estimates were aggregated across drugs, accounting for the co-occurrence of resistance to multiple drugs. Error bars show 95% uncertainty intervals. GBD=Global Burden of Diseases, Injuries, and Risk Factors Study. Figure adapted from (Murray et al., 2022).

APPENDIX 2: NUMBER OF STUDIES ON ANTIBIOFILM ACTIVITY

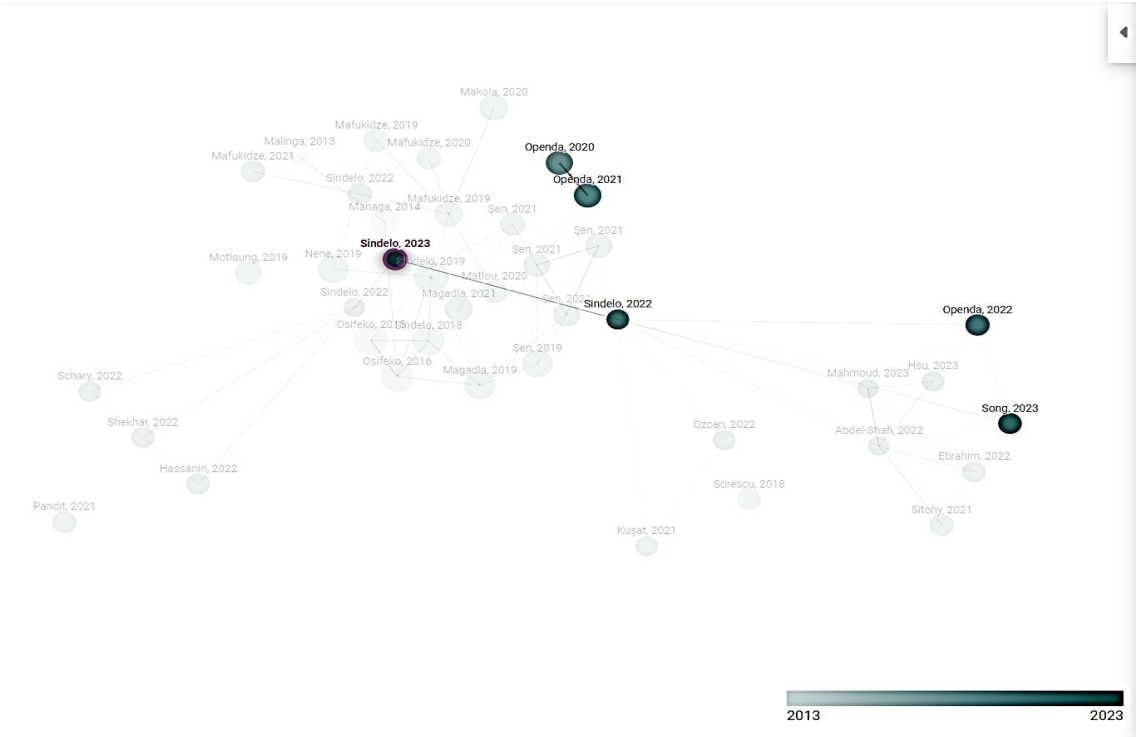

The image shows the number of studies on the antibacterial and antibiofilm activity of Schiff base reported during the last 10 years, the colored green reports represent the antibiofilm activity, while the transparent reports are the total number of studies on antibacterial activity elaborated by different authors (Conected Pappers, 2023).

APPENDIX 3: FLUORESCENCE MICROSCOPY OF THE BEST INHIBITORY COMPOUNDS

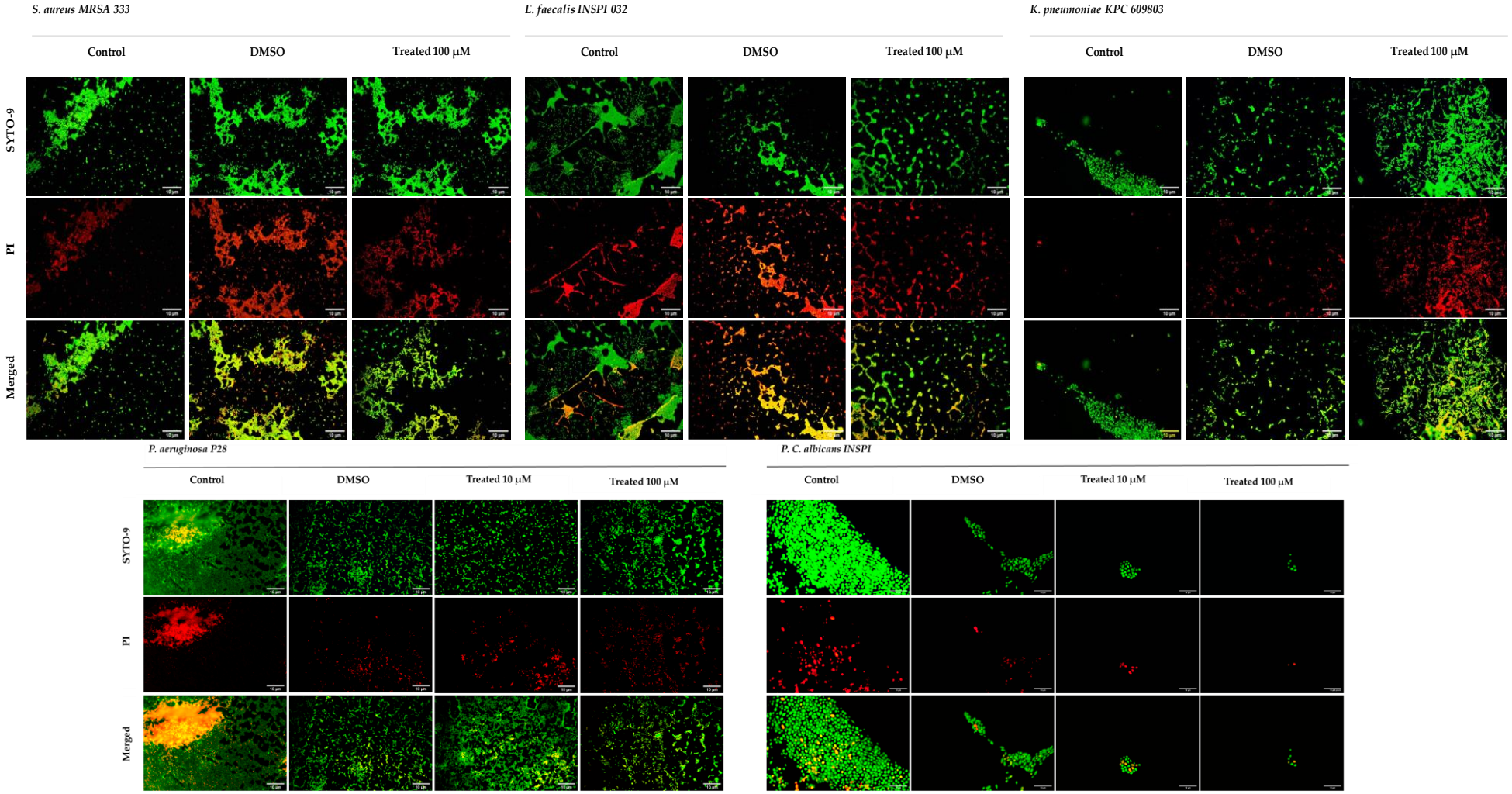

Biofilms after inhibition processes against *S. aureus* MRSA 333, *K. pneumoniae* KPC 609803, *P. aeruginosa* P28, *E. faecalis* INSPI 032, and *C. albicans* INSPI with the best Schiff bases 3a, 3d, and 3h compounds by fluorescence microscopy using live/dead staining. The original image was magnified to 1:10 to observe the biofilm cells and compare the total live and dead cells. An Olympus bx50 microscope was used at 100x magnification, and images were obtained with amscope software and merged with Fiji-imagej software.